

Minerva Access is the Institutional Repository of The University of Melbourne

Author/s:

King, NE;Courtney, JM;Brown, LS;Fortune, AJ;Blackburn, NB;Fletcher, JL;Cashion, JM;Talbot, J;Pébay, A;Hewitt, AW;Morris, GP;Young, KM;Cook, AL;Sutherland, BA

Title:

Induced pluripotent stem cell derived pericytes respond to mediators of proliferation and contractility

Date:

2024-12-01

Citation:

King, N. E., Courtney, J. M., Brown, L. S., Fortune, A. J., Blackburn, N. B., Fletcher, J. L., Cashion, J. M., Talbot, J., Pébay, A., Hewitt, A. W., Morris, G. P., Young, K. M., Cook, A. L. & Sutherland, B. A. (2024). Induced pluripotent stem cell derived pericytes respond to mediators of proliferation and contractility. *Stem Cell Research and Therapy*, 15 (1), <https://doi.org/10.1186/s13287-024-03671-x>.

Persistent Link:

<https://hdl.handle.net/11343/353163>

License:


[CC BY](#)

RESEARCH

Open Access



Induced pluripotent stem cell derived pericytes respond to mediators of proliferation and contractility

Natalie E. King¹, Jo-Maree Courtney¹, Lachlan S. Brown¹, Alastair J. Fortune², Nicholas B. Blackburn², Jessica L. Fletcher², Jake M. Cashion¹, Jana Talbot³, Alice Pébay^{4,5}, Alex W. Hewitt^{1,2,4,5,6}, Gary P. Morris¹, Kaylene M. Young², Anthony L. Cook³ and Brad A. Sutherland^{1*} 

Abstract

Background Pericytes are multifunctional contractile cells that reside on capillaries. Pericytes are critical regulators of cerebral blood flow and blood–brain barrier function, and pericyte dysfunction may contribute to the pathophysiology of human neurological diseases including Alzheimers disease, multiple sclerosis, and stroke. Induced pluripotent stem cell (iPSC)-derived pericytes (iPericytes) are a promising tool for vascular research. However, it is unclear how iPericytes functionally compare to primary human brain vascular pericytes (HBVPs).

Methods We differentiated iPSCs into iPericytes of either the mesoderm or neural crest lineage using established protocols. We compared iPericyte and HBVP morphologies, quantified gene expression by qPCR and bulk RNA sequencing, and visualised pericyte protein markers by immunocytochemistry. To determine whether the gene expression of neural crest iPericytes, mesoderm iPericytes or HBVPs correlated with their functional characteristics in vitro, we quantified EdU incorporation following exposure to the key pericyte mitogen, platelet derived growth factor (PDGF)-BB and, contraction and relaxation in response to the vasoconstrictor endothelin-1 or vasodilator adenosine, respectively.

Results iPericytes were morphologically similar to HBVPs and expressed canonical pericyte markers. However, iPericytes had 1864 differentially expressed genes compared to HBVPs, while there were 797 genes differentially expressed between neural crest and mesoderm iPericytes. Consistent with the ability of HBVPs to respond to PDGF-BB signalling, PDGF-BB enhanced and a PDGF receptor-beta inhibitor impaired iPericyte proliferation. Administration of endothelin-1 led to iPericyte contraction and adenosine led to iPericyte relaxation, of a magnitude similar to the response evoked in HBVPs. We determined that neural crest iPericytes were less susceptible to PDGFR beta inhibition, but responded most robustly to vasoconstrictive mediators.

Conclusions iPericytes express pericyte-associated genes and proteins and, exhibit an appropriate physiological response upon exposure to a key endogenous mitogen or vasoactive mediators. Therefore, the generation of functional iPericytes would be suitable for use in future investigations exploring pericyte function or dysfunction in neurological diseases.

*Correspondence:

Brad A. Sutherland

brad.sutherland@utas.edu.au

Full list of author information is available at the end of the article



© The Author(s) 2024. **Open Access** This article is licensed under a Creative Commons Attribution 4.0 International License, which permits use, sharing, adaptation, distribution and reproduction in any medium or format, as long as you give appropriate credit to the original author(s) and the source, provide a link to the Creative Commons licence, and indicate if changes were made. The images or other third party material in this article are included in the article's Creative Commons licence, unless indicated otherwise in a credit line to the material. If material is not included in the article's Creative Commons licence and your intended use is not permitted by statutory regulation or exceeds the permitted use, you will need to obtain permission directly from the copyright holder. To view a copy of this licence, visit <http://creativecommons.org/licenses/by/4.0/>. The Creative Commons Public Domain Dedication waiver (<http://creativecommons.org/publicdomain/zero/1.0/>) applies to the data made available in this article, unless otherwise stated in a credit line to the data.

Keywords Induced pluripotent stem cells (iPSCs), Pericytes, Human brain vascular pericytes (HBVPs), Proliferation, Platelet-derived growth factor BB (PDGF-BB), Platelet-derived growth factor receptor β (PDGFR β), Contractility, Adenosine, Endothelin-1

Background

Pericytes are contractile cells that reside within the capillary bed. In the cerebrovasculature, pericytes are essential regulators of cerebral blood flow and contribute to blood–brain barrier formation and function [1]. Pericyte dysfunction may contribute to the pathophysiology of neurological diseases including Alzheimer’s disease, stroke, and multiple sclerosis [1, 2]. For example, the aggregation of amyloid- β , a key protein associated with Alzheimer’s disease pathology, induces pericyte constriction by modulating the endothelin-1 receptor signalling pathway [3]. Furthermore, pericytes die during stroke, in a way that constricts capillaries and prevents tissue reperfusion even after large vessels reopen—a phenomenon known as ‘no-reflow’ [4]. In addition, pericytes can also have reparative properties as it has been shown that activation of the pericyte PDGFR β signalling pathway can facilitate repair following a stroke, by supporting fibrotic scar formation [5].

iPSC-derived pericytes (iPericytes) are increasingly used in place of primary pericyte lines to model pericyte function in health and disease [6–11]. iPericytes have several advantages over primary pericyte lines, as they can be derived from iPSCs reprogrammed from individuals of various genetic backgrounds and disease diagnoses [12], allowing them to be used for basic biological studies as well as disease modelling or phenotyping. It is also possible to co-culture iPericytes with cells derived from the same iPSC line, to model the neurovascular unit (NVU) [13]. Finally, iPericytes may be compatible with personalised medicine approaches as they could be returned to the donor without immune rejection. Indeed, a recent study showed pericytes derived from mouse embryo cells could improve microcirculation in animal models of Alzheimer’s disease [14], however, this technique is yet to be performed in iPSCs derived from the same donor.

There are several published methods for iPericyte differentiation [7–11, 15, 16]. One describes a 10-day method for generating iPericytes of two developmental lineages: neural crest or mesoderm iPericytes [17]. The iPericytes had morphological features that were consistent with primary pericyte lines and expressed key pericyte markers including PDGFR β , alanyl aminopeptidase (CD13) and neuron-gial antigen 2 (NG2) [17]. While the expression of key pericyte markers is promising, it is essential to understand the functional capacity of

iPericytes relative to primary pericyte lines. iPericytes can increase endothelial cell expression of BBB markers in co-culture, improve trans-endothelial electrical resistance (TEER) and enhance the formation of 3D endothelial cell tubes [7, 9, 10, 15, 17]. However, the proliferative and contractile functions of iPericytes in response to known mediators have not been explored extensively, and a side-by-side comparison of iPericytes and primary HBVPs is also lacking.

In this study, we therefore aimed to characterise the gene expression profiles, and proliferative and contractile properties of neural crest and mesoderm iPericytes and compared them to HBVPs. We compared the PDGF-BB and PDGFR β -mediated mitogenic response of neural crest and mesoderm iPericytes, and quantified cell area change in response to the vasoconstrictor, endothelin-1 and vasodilator, adenosine. We report that iPericytes have functional PDGFR β signalling, capable of mediating proliferation. Furthermore, iPericyte area changes in response to endothelin-1 and adenosine. iPericytes are functionally similar to HBVPs, making them suitable for use in *in vitro* assays and for disease modelling.

Materials and methods

Pluripotent stem cell lines

The TOB-00220 iPSC line (from an apparently healthy 67 year-old male donor) [18] was cultured to generate mesoderm and neural crest iPericytes with approval from the University of Tasmania Human Research Ethics Committee (Project H26563). Additional healthy control iPSC lines were used as specified in text: MNZTASi019-A (from a 53 year-old female donor); MNZTASi021-A (76 year-old male donor), and MNZTASi022-A (56 year-old female donor) were purchased from the MS Stem biobank (Menzies Institute for Medical Research, Hobart, Tasmania, Australia). MS Stem iPSCs were generated and characterised as previously described [19, 20] with approval from the University of Tasmania Human Research Ethics Committee (Project H16915). All iPSC lines were shown to have karyotypically normal karyograms within 10 passages of use for experiments and were used between passage 5–35.

Pluripotent stem cell culture

iPSCs were grown on Matrigel (Merck, cat.#354277) coated plates in mTeSR+ cell culture medium (Stem Cell

Technologies, cat.#05825) maintained at 37 °C in a 20% O₂/5% CO₂ humidified incubator. The culture medium was exchanged every 2 days, and iPSCs were cultured to generate large colonies (~60–100 µm diameter) with distinct round edges. iPSC colonies were passaged using Versene Solution (Gibco, cat.#15040066).

Differentiation of iPSCs into mesoderm or neural crest iPericytes

iPSCs were differentiated to produce iPericytes by adapting a previously published protocol [17] (see Additional file 1: Fig. S1). Induction into mesoderm iPericytes was achieved by culturing in Mesoderm Induction Media (Stem Cell Technologies, cat.#05221). Induction into neural crest iPericytes was achieved by culturing in DMEM/F-12 plus GlutaMAX (ThermoFisher Scientific, cat.#10565018) supplemented with 0.5% (v/v) Bovine Serum Albumin (Sigma Aldrich, cat.#A9418), 2% (v/v) B27 (ThermoFisher Scientific, cat.#17504-044) and 3 µM CHIR 99021 (GSK3 inhibitor; Tocris Bioscience, cat.#TB4423-GMP). Medium was exchanged daily for 5 days before it was replaced with Complete Pericyte Medium (CPM, ScienCell Research Laboratories, cat.#1201), which was exchanged daily for a further 5 days. After 10-days, the resulting iPericytes were maintained as outlined below.

Pericyte culture

Human brain vascular pericytes (HBVPs, ScienCell, cat.#1200) and iPericytes were grown in CPM which was replaced every second day. Pericytes were passaged at 60–90% confluence by washing with Dulbecco's phosphate buffered saline without magnesium or calcium (DPBS^{-/-}, ThermoFisher Scientific, cat.#14190-144) prior to treatment with TrypLE Express (ThermoFisher Scientific, cat.# 12604013). Pericytes were passaged and the cells allowed to adhere for ≥ 16 h prior to commencing experiments. All HBVPs and iPericytes were used between passage 2–8.

Real time qPCR

To quantify the expression of pericyte-associated genes in HBVPs, iPSCs, mesoderm iPericytes or neural crest iPericytes using real time quantitative polymerase chain reaction (qPCR), cells were grown to 95% confluence in 6-well plates (Interpath, cat.#657160). Cells were collected from n = 3 wells per cell type of the same differentiation, and RNA was extracted using an RNeasy mini kit (Qiagen, cat.#74104), following the manufacturer's recommendations. RNA concentration was quantified using a NanoDrop (ND-1000, ThermoFisher Scientific) and RNA quality was evaluated in a subset of samples using an Agilent 4200 Tape Station system (cat.#G2991AA)

with an RNA ScreenTape Ladder (Agilent, cat.#5067-5578), following the manufacturer's instructions. cDNA synthesis was performed using the High Capacity cDNA Reverse Transcription Kit (ThermoFisher Scientific, cat.#4368814). For reverse transcription a SuperCycler Trinity (Kyratec, cat.#SC-200) was set to the program: step 1–25 °C, 10 min; step 2–37 °C, 120 min; step 3–85 °C, 5 min; step 4–4 °C, infinity. 200 ng of cDNA was added to the TaqMan Fast Advanced Master Mix (ThermoFisher Scientific, cat.#4444557) and TaqMan primers for mRNAs of interest for each 20 µL qPCR reaction. MicroAmp Optical 96 Well Reaction Plates (ThermoFisher, cat.#N8010560) were placed in a QuantStudio 3 (ThermoFisher Scientific, cat.#A28567) operating the following program: step 1–50 °C, 2 min; step 2–95 °C, 2 min; step 3–95 °C, 1 s then 60 °C, 20 s (X 40). Raw data were exported into the QuantStudio Design and Analysis Software (v1.5.1, Applied Biosystems) to calculate Cycle threshold (Ct) values for each sample. Delta Ct values, delta delta Ct values and 2^{-delta delta Ct} were calculated in Microsoft excel, using *HPRT1* as a housekeeping gene. Primers included: *CSPG4* (Hs00361541_g1, ThermoFisher Scientific, cat.# 4331182), *OCT4* (Hs01895061_u1, ThermoFisher Scientific, cat.# 4331182), *NANOG* (Hs04399610_g1, ThermoFisher Scientific, cat.# 4331182), *ACTA2* (Hs00426835_g1, ThermoFisher Scientific, cat.#4331182), *PDGFRB* (Hs01019589_m1, ThermoFisher Scientific, cat.# 4331182) and *HPRT1* (Hs02800695_m1, ThermoFisher Scientific, cat.# 4331182).

Immunocytochemistry

For immunocytochemical studies, HBVPs, mesoderm iPericytes and neural crest iPericytes were plated in Greiner 24 Well Plates (Interpath, cat.#662160X) on glass coverslips (18 mm number 1 glass, Menzel-Glaser) in 12 well plates preincubated with poly-L-lysine (0.01% v/v in sterile water, Sigma-Aldrich, Merck, #25988-63-0) for 1.5 h at 37 °C, and grown to >50% confluency. Media was removed and cells were fixed by immersion in ice-cold methanol (100%) for 10 min prior to washing with ice-cold PBS (Gibco, cat.#18912014). Cells were washed thrice with 0.1% (v/v) tween-20/PBS and permeabilised with PBS containing Triton X-100 (0.3%v/v, Sigma Aldrich, #1002116296) (for αSMA only), washed thrice again, then incubated in Serum Free Protein Block (DAKO, cat.#X0909) for 1 h at 21 °C. Primary antibodies (goat anti-PDGFRβ, R&D Systems AF385, RRID:AB_777165; rabbit anti-CD13, Abcam Ab108310, RRID:AB_10866195; rabbit anti-αSMA, Abcam Ab5694, RRID:AB_2223021) were diluted 1:500 in Antibody Diluent (DAKO, cat.#S302283-2) and applied to cells overnight at 4 °C. Cells were washed thrice in 0.1% (v/v) tween-20/PBS before applying secondary antibody (Alexa

Fluor 488-conjugated Donkey anti-rabbit, ThermoFisher Scientific, cat.# A-21206) diluted 1:1000 in Antibody Diluent for 1 h at 21 °C in the dark. Cells were washed thrice in PBS and incubated with 4',6-diamidino-2-phenylindole (DAPI) (Sigma, #D9542) diluted 1:10,000 in PBS for 5 min. Cells were imaged at 20× using an Olympus FV3000 Super Resolution confocal laser scanning microscope (Olympus, Japan).

RNA sequencing, data processing and differential gene expression analysis

Samples containing >10 ng/μl RNA with a RIN of >8 were sent to the Australian Genome Research Facility for bulk RNA sequencing. Libraries were generated using an Illumina Stranded mRNA workflow with polyA capture. RNA sequencing, processing of raw sequencing data, and quantification of gene expression are described in the supplementary methods. Differential gene analysis, principal components analysis (PCA), gene ontology analysis and heatmap generation were performed using DESeq2 and other tools as described in supplementary methods.

Proliferation assay

An EdU assay was used, as described previously [21], to quantify proliferation in mesoderm or neural crest iPericytes compared to HBVPs. Briefly, pericytes were plated in 96 well plates (Interpath, cat.#655180) and grown to 50% confluency (~5000 cells per well). CPM was replaced with either: CPM containing the complete array of pericyte growth factors, incomplete pericyte media (PM) which did not contain any growth factors, PM supplemented with 100 ng/mL PDGF-BB (Sigma Aldrich, SRP3138) or PM supplemented with 100 ng/mL PDGF-BB with either 0.1 μM, 10 μM or 100 μM imatinib (Sapphire Bioscience, 00022120). Pericytes were cultured for 24 h prior to fixation by immersion in 4% (w/v) PFA in PBS for 15 min at 21 °C. EdU incorporation into the DNA was revealed using a Click-iT EdU Cell Proliferation Kit (Invitrogen, cat.#C10340) following the manufacturer's instructions, and the nuclei of all cells were identified by staining with DAPI. EdU and DAPI labelling was visualised and imaged at 20× magnification using a Nikon Ti2 SRRF microscope. A region of interest spanning 3 mm² (20× magnification, 3×3) was defined, imaged and stitched to create a single image spanning the region of interest for quantification. QuPath V0.2.3 was used to identify total cells from the DAPI channel as well as proliferative cells from the EdU channel using techniques previously described [22]. Briefly, channel colours (DAPI, EdU) were set for all images as a batch using the script "Channels and colours.groovy", described previously [22]. The rectangle annotation tool was used to draw a ROI around each image using the script "Select all ROI.

groovy". DAPI and EdU positive cells were detected using the Positive Cell Detection tool using the script "EDU Analysis". Proliferation was calculated as:

$$\%EdU \text{ positive cells} = \left(\frac{EdU \text{ positive cells}}{DAPI \text{ positive cells}} \right) \times 100.$$

Contraction assay

An xCelligence Real-Time cell analysis electrical impedance assay was used, as previously published [23], to quantify contractility in mesoderm or neural crest iPericytes compared to HBVPs. 5000 pericytes were plated in each well of an E-Plate (ACEA Biosciences, cat.# 05469830001), with 200 μL of CPM. After ~16 h, cells were above 50% confluence and CPM was replaced with CPM alone (control) or CPM containing 50 nM endothelin-1 or 10 μM adenosine, concentrations as used previously [23, 24] (n=4 wells per condition) and the plate was placed in the xCelligence system. The xCelligence system measures the relative impedance of electron flow expressed as arbitrary 'cell index' units as an indicator of cell area (Additional file 1: Fig. S6). Cell index was measured every minute for 2 h at 37 °C and 5% CO₂. The normalised cell index value was calculated by normalising the raw cell index values to the cell index value at baseline t=0 as described previously [25]. Area under the curve (AUC) was calculated using GraphPad prism for the normalised cell index graphed over the first 20 min following drug exposure. Change (Δ) in cell index was calculated at the maximum point of contraction in each well (Maximum Δ Cell Index) using the equation:

$$\begin{aligned} \text{Max } \Delta \text{ Cell Index} = & \text{baseline cell index}(1) \\ & - \text{cell index at maximum contraction.} \end{aligned}$$

Change in cell index was also calculated after 2 h (Δ Cell index after 2 h) to determine the maintenance of contraction after 2 h using the equation:

$$\Delta \text{Cell index after 2 h} = \text{baseline cell index}(1) - \text{cell index at 2 h.}$$

See Additional file 1: Fig. S6 for more details about the xCelligence system and calculations.

Statistical analyses

Statistical analyses were performed using Prism 9.3.1 (GraphPad, USA) except for RNA-seq data where DESeq2 and R were used (see supplementary methods for details about RNA-seq analysis). Prior to performing statistical comparisons in Prism, outliers were removed using the ROUT's outlier test (Q=1%). Each data set was tested for normality of residuals using the Shapiro–Wilk test, and either a Y=Log(Y) transformation was performed to enable parametric testing, or data

sets were analysed with non-parametric Mann–Whitney U or Kruskal–Wallis tests. To compare qPCR data generated from iPSCs and iPericytes, we performed a one-way ANOVA with a Dunnett’s multiple comparisons test or Sidak’s multiple comparisons test. To determine the effect of experimental conditions on proliferation, we performed a one-way ANOVA, with differences between conditions versus control determined using a Dunnett’s multiple comparisons test. For the contraction assay, we performed a two-way ANOVA to determine the effect of cell type (mesoderm iPericytes, neural crest iPericytes, or HBVPs) or treatment (control, endothelin-1 or adenosine) on cell index parameters, followed by a Tukey’s multiple comparison test for pair-wise comparisons. A $p < 0.05$ was considered statistically significant. Statistical tests and results for each analysis are reported in the figure legends.

Results

iPericytes display characteristic pericyte morphology and express canonical pericyte markers

To determine whether iPericytes have the morphological characteristics of pericytes, we collected phase contrast micrographs of mesoderm and neural crest iPericytes and HBVPs and assessed the morphological features of each cell type. Throughout the differentiation process, mesoderm and neural crest iPericytes possessed similar morphological features (Additional file 1: Fig. S2). After differentiation, mesoderm and neural crest iPericytes had elongated fusiform cell bodies, that were similar in morphology to HBVPs (Fig. 1A, Additional file 1: Fig. S2). In vitro, HBVPs adopt several morphological phenotypes, that relate to different contractile “subsets” [24]. Mesoderm and neural crest iPericytes cultures also contained each of these morphological phenotypes (Additional file 1: Fig. S3) and in proportions similar to those reported for HBVPs [24]. To determine whether iPericytes express classical pericyte markers, we isolated RNA and generated cDNA to conduct a qPCR analysis. iPericytes expressed mRNAs that are integral to pericyte function, particularly: *PDGFRB*, which encodes the PDGFR β protein; *CSPG4* which encodes NG2 proteoglycan, and *ACTA2*

which encodes alpha-smooth muscle actin (α SMA). Compared to iPSCs, HBVPs, mesoderm and neural crest iPericytes expressed significantly higher levels of *CSPG4* (HBVP, $p = 0.0020$; neural crest iPericytes, $p < 0.0001$; mesoderm iPericytes, $p < 0.0001$). Mesoderm and neural crest iPericytes, but not HBVPs also expressed more *PDGFRB* (HBVP, $p = 0.1387$; neural crest iPericytes, $p < 0.0001$, mesoderm iPericytes, $p = 0.0002$) and *ACTA2* (HBVP, $p = 0.1145$; neural crest iPericytes, $p = 0.0051$; mesoderm iPericytes, $p = 0.0447$) mRNA than iPSCs (Fig. 1B). There were also differences between all three pericyte lines in expression of *CSPG4* (HBVP vs. neural crest iPericytes, $p < 0.0001$; HBVP vs. mesoderm iPericytes, $p < 0.0001$; neural crest iPericytes vs. mesoderm iPericytes, $p < 0.0001$) and *PDGFRB* (HBVP vs. neural crest iPericytes, $p < 0.0001$; HBVP vs. mesoderm iPericytes, $p = 0.0047$; neural crest iPericytes vs. mesoderm iPericytes, $p = 0.0002$), but not *ACTA2*. Conversely, HBVPs, neural crest and mesoderm iPericytes expressed pluripotency genes at a very low level; expressing less *OCT4* (HBVP, $p < 0.0001$; neural crest iPericyte, $p < 0.0001$; mesoderm iPericyte, $p < 0.0001$) and *NANOG* (HBVP, $p < 0.0001$; neural crest iPericyte, $p < 0.0001$; mesoderm iPericyte, $p < 0.0001$) mRNA than iPSCs (Fig. 1C).

To extend these mRNA expression findings, we performed immunocytochemistry to determine whether iPericytes expressed proteins synonymous with pericyte identity: PDGFR β and CD13. Mesoderm and neural crest iPericytes displayed similar patterns of expression of PDGFR β and CD13 compared to HBVPs (Fig. 1D). Quantification of the proportion of iPericytes expressing pericyte markers revealed that the vast majority of cells had positive labelling for PDGFR β (HBVP 93%, mesoderm iPericyte 96%, and neural crest iPericyte 97%) and CD13 (HBVP 95%, mesoderm iPericyte 95%, and neural crest iPericyte 88%, suggesting these cultures were highly enriched for pericyte markers (Additional file 1: Fig. S4). Mesoderm and neural crest iPericytes also expressed the contractile protein α SMA similar to HBVPs (Fig. 1D). Overall, these data show that iPericytes are morphologically similar to HBVPs, express mRNAs and proteins that

(See figure on next page.)

Fig. 1 iPericytes are morphologically similar to HBVPs and express pericyte markers. **A** Phase contrast bright 4 \times magnification images of iPSCs, HBVPs, mesoderm iPericytes and neural crest iPericytes. Scale = 200 μ m. **B–C** Fold change gene expression measured by qPCR of pericyte genes *PDGFRB*, *CSPG4*, *ACTA2* (B) and pluripotency genes *OCT4* and *NANOG* (C) by iPSCs, neural crest iPericytes, mesoderm iPericytes and HBVPs ($n = 3$ per cell type). Data are normalised to HBVP cells, and comparisons were made using a one-way ANOVA: *PDGFRB* ($F(3, 8) = 103.1, p < 0.0001$), *CSPG4* ($F(3, 8) = 4671, p < 0.0001$), *ACTA2* ($F(3, 8) = 9.340, p < 0.0054$), *OCT4* ($F(3, 8) = 1686, p < 0.0001$) and *NANOG* ($F(3, 8) = 606.4, p < 0.0001$). Post-hoc comparisons performed using Dunnett’s multiple comparisons test: * $p < 0.05$; ** $p < 0.01$; *** $p < 0.001$; **** $p < 0.0001$. Data are shown as mean \pm SD. **D** Immunocytochemistry showing expression of proteins PDGFR β , CD13, and α SMA (green) by HBVP, mesoderm iPericytes and neural crest iPericytes. Nuclei counter-stained with DAPI (blue). Scale = 10 μ m

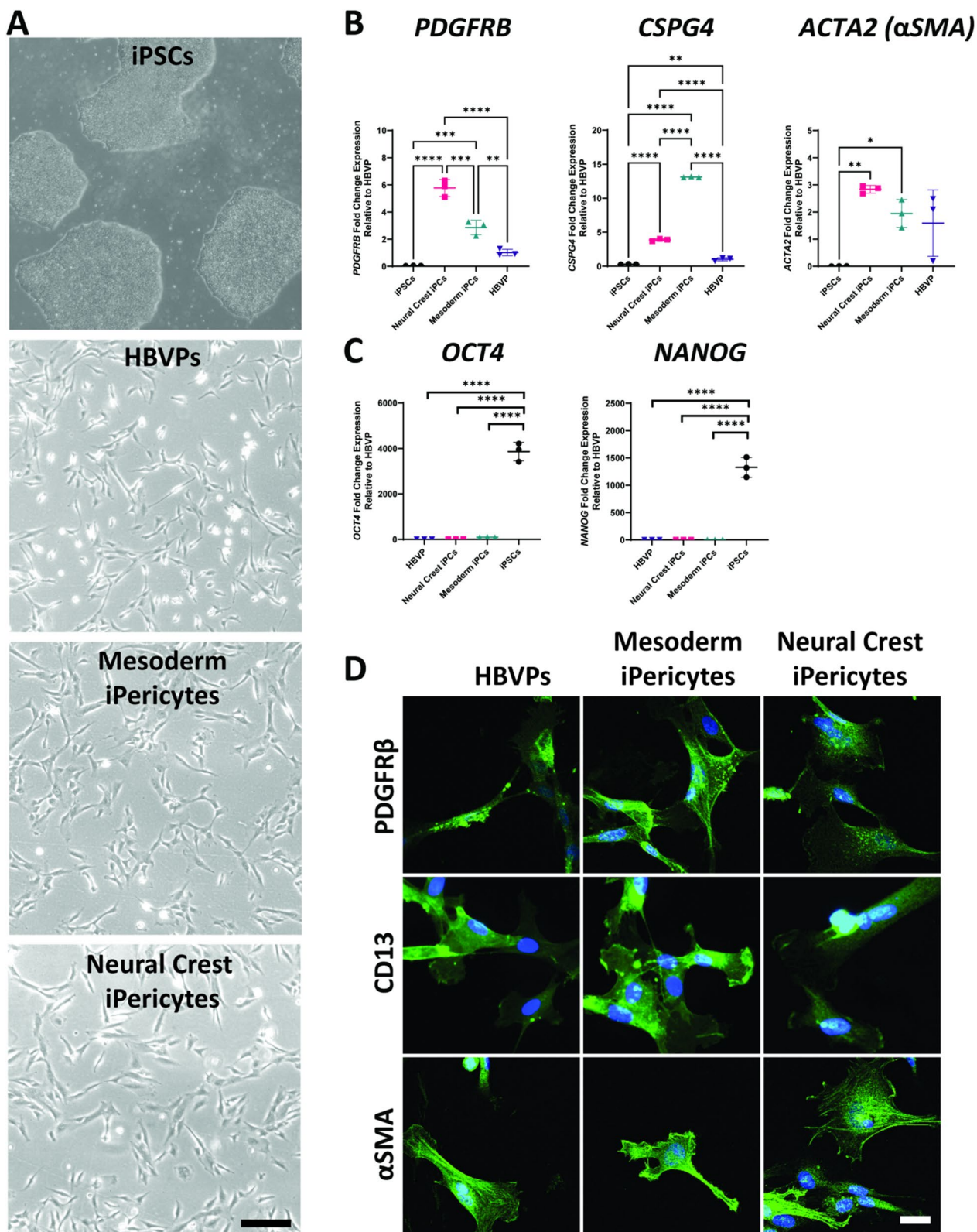


Fig. 1 (See legend on previous page.)

are consistent with pericyte identity, and expression is highly enriched across the whole culture.

Mesoderm and neural crest iPericytes have different gene expression profiles

To identify differences in gene expression between mesoderm and neural crest iPericytes, and to determine how similar these cells are to HBVPs, we performed bulk RNA sequencing. A PCA revealed that the majority of the variance was accounted for through the difference between HBVPs and iPericytes regardless of lineage (PC1: 78% variance), whereas PC2 (12% variance) accounted for the variation between neural crest and mesoderm iPericytes (Fig. 2A). Differential gene expression analysis was used to explore differences between HBVPs and iPericytes (Fig. 2B–D), or neural crest and mesoderm iPericytes (Fig. 2E–G). There were a substantial number of differentially expressed genes between HBVPs and iPericytes, with 984 genes upregulated and 880 genes downregulated in iPericytes compared to HBVP (Fig. 2B). This is also reflected in the heat map with clear differences in gene expression between HBVPs and iPericytes, regardless of lineage (Fig. 2C). Gene ontology analysis of differentially expressed genes between HBVPs and iPericytes showed enrichment for genes related to tissue development, cellular division, morphology, extracellular matrix production and protein binding (Fig. 2D).

Next, we assessed for differential gene expression between mesoderm and neural crest iPericytes, which revealed 458 genes upregulated and 339 genes downregulated in neural crest iPericytes compared to mesoderm iPericytes (Fig. 2E). Visualisation of these differentially expressed genes via a heat map demonstrated the separation between mesoderm iPericytes and neural crest iPericytes (Fig. 2F). Gene ontology analysis showed enrichment for genes related to tissue development, extracellular matrix production, DNA/RNA processing and growth factor binding and activity (Fig. 2G). These differences could reflect changes in cellular function between mesoderm and neural crest iPericytes and HBVPs.

Validation of the mesoderm iPericyte differentiation protocol using multiple iPSC lines

To confirm that iPericyte differentiation is highly reproducible, multiple unrelated iPSC lines (MNZTASi019-A, MNZTASi021-A, and MNZTASi022-A) were cultured and used to generate mesoderm iPericytes. RNA was collected from the iPSCs and the iPericytes for bulk RNA sequencing. PCA of the gene expression profile of the iPSCs and mesoderm iPericytes revealed that each cell type (iPSCs and iPericytes) clustered separately along the first principal component, accounting for 93% of sample variation (Fig. 3A). Variation between replicates accounted for only 5% of sample variation, showing a remarkable similarity between replicates (Fig. 3A). We then selected genes associated with iPSC, pericyte, endothelial cell, microglia, oligodendrocyte progenitor cell (OPC), oligodendrocyte, astrocyte, or neuronal identity, and generated a heat map of gene expression for each iPSC line and the corresponding iPericytes (Fig. 3B). Regardless of donor, iPericytes had successfully downregulated the pluripotency genes *NANOG*, *POU5F1* and *SOX2*, and upregulated pericyte-associated genes, including *PDGFRB*, *CSPG4*, *ANPEP* and *ACTA2* (Fig. 3B). Gene expression was consistent across iPericytes generated from different iPSC lines (Fig. 3B). Importantly, iPericytes did not express genes synonymous with other neurovascular cell types (Fig. 3B). These data indicate this differentiation protocol can be applied to distinct iPSC lines and produce iPericytes with a consistent mRNA expression profile.

PDGFR β signalling promotes iPericyte proliferation

mRNA expression differences between HBVPs and iPericytes could influence their capacity to respond to environmental signals, and so we next compared the proliferative capacity of these cells. A key ligand-receptor pathway that pericytes utilise for survival and proliferation is the PDGFR β signalling pathway [21]. We exposed HBVPs or iPericytes to basal pericyte medium alone (PM) or PM containing the PDGFR β ligand,

(See figure on next page.)

Fig. 2 iPericytes derived through different lineage pathways have differential expression of genes. **A** PCA analysis showing separate clustering of mesoderm iPericytes, neural crest iPericytes and HBVPs (n = 6 for HBVPs, n = 3 for mesoderm or neural crest iPericytes). **B** Volcano plots showing upregulated and downregulated genes in iPericytes compared to HBVPs that met the log fold change threshold of 1. **C** Heat map showing differentially expressed genes in iPericytes compared to HBVPs. **D** Gene ontology analysis of key biological processes, cellular compartments and molecular function associated with 1,864 differentially expressed genes between iPericytes and HBVPs. **E** Volcano plots showing upregulated and downregulated genes in neural crest iPericytes compared to mesoderm iPericytes. **F** Heat map showing differentially expressed genes in neural crest iPericytes compared to mesoderm iPericytes. **G** Gene ontology analysis of key biological processes, cellular compartments and molecular function associated with 797 differentially expressed genes between neural crest iPericytes and mesoderm iPericytes

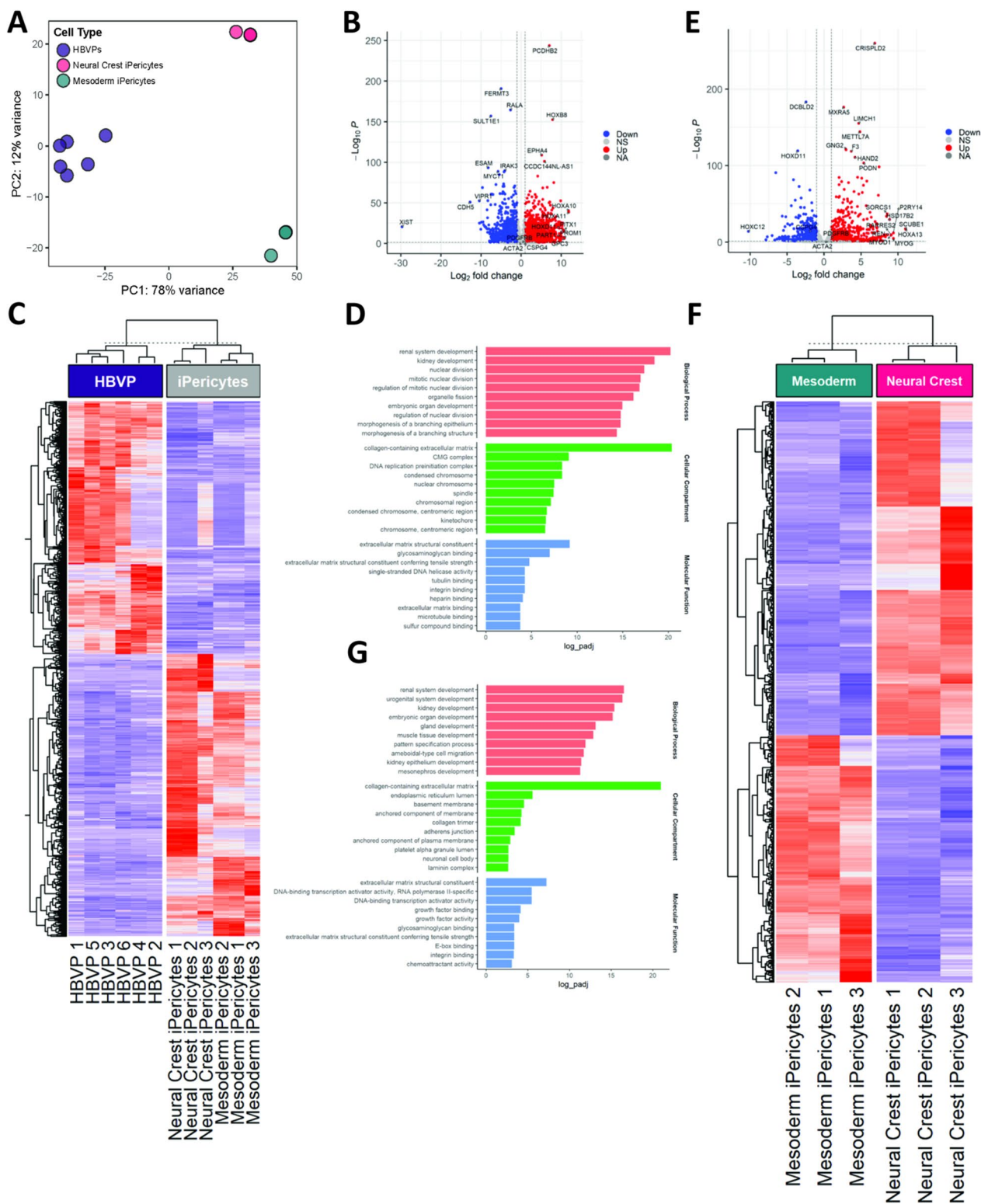


Fig. 2 (See legend on previous page.)

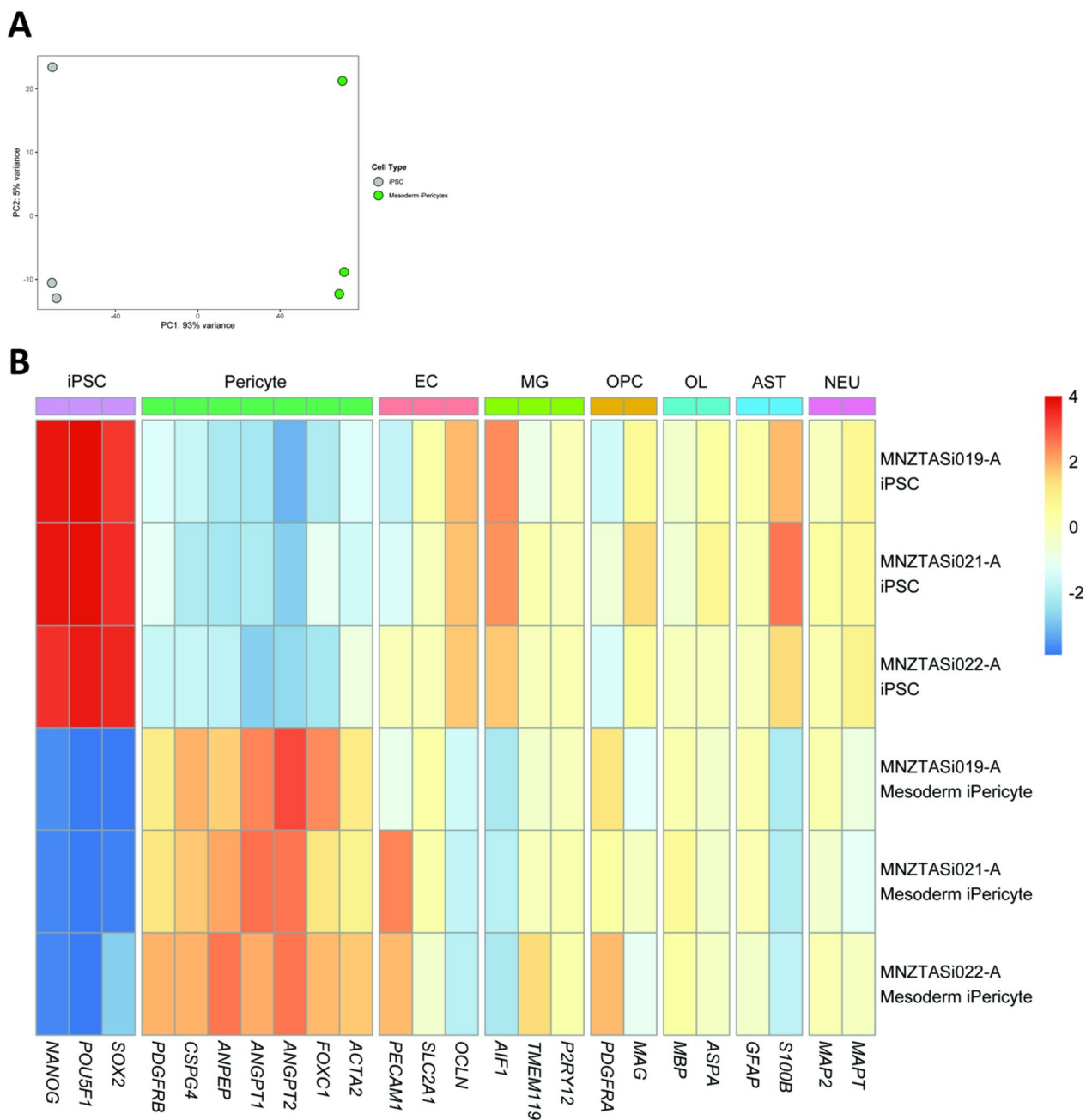


Fig. 3 Mesoderm iPericytes from multiple cell lines have similar mRNA expression. **A** Principal components analysis showing separate clustering of mesoderm iPericytes and iPSCs from $n = 3$ different cell lines. **B** Heat map showing relative expression levels in iPSCs and mesoderm iPericytes of key genes typically expressed by iPSCs, pericytes, endothelial cells (EC), microglia (MG), oligodendrocyte precursor cells (OPCs), oligodendrocytes (OL), astrocytes (AST) and neurons (NEU). Warmer colours indicate higher expression, cooler colours indicate lower expression

PDGF-BB (100 ng/ml), in the presence of the thymidine analogue, EdU, as previously described [21]. The addition of PDGF-BB increased the proportion of HBVPs and iPericytes that incorporated EdU over a 24 h period, indicative of increased proliferation (Fig. 4A, B, Additional file 1: Fig. S5; HBVP, $p < 0.0001$; neural crest iPericytes, $p = 0.01$; mesoderm iPericytes, $p < 0.0001$).

The magnitude of response to PDGF-BB was similar between all three pericyte lines. Similar results were observed when complete pericyte media (CPM), containing specialised pericyte growth supplement (SciCell, USA), was used compared to PM (Fig. 4B). These results indicate that iPericytes can proliferate in response to the pericyte growth factor PDGF-BB.

To confirm that the proliferative response was mediated by PDGFR β , HBVP and iPericyte proliferation was assessed in the presence of imatinib. In pericytes, imatinib inhibits PDGFR β phosphorylation to prevent proliferation [21]. In HBVPs and iPericytes, imatinib produced a dose dependent inhibition of PDGF-BB-induced proliferation (Fig. 4C, Additional file 1: Fig. S5). For HBVPs, 0.01 μ M imatinib did not alter proliferation ($p=0.9851$), while 10 μ M imatinib and 100 μ M imatinib significantly reduced proliferation by 31% and 96% of PDGF-BB alone, respectively ($p<0.0001$). Mesoderm iPericytes also failed to respond to 0.01 μ M imatinib (51%, $p=0.6517$), while 10 μ M and 100 μ M imatinib significantly reduced proliferation to 37% and 8% of PDGF-BB alone, respectively ($p<0.0001$). Neural crest iPericytes were less sensitive to PDGFR β blockade, as neither 0.01 μ M ($p=0.9723$) or 10 μ M ($p=0.3121$) altered PDGF-BB-induced proliferation. However, 100 μ M imatinib significantly reduced the proliferation rate to 11% of that recorded for PDGF-BB alone ($p=0.0009$). These findings indicate that neural crest iPericytes are less sensitive than mesoderm iPericytes or HBVPs to PDGFR β inhibition.

To determine why neural crest iPericytes have altered susceptibility to PDGFR β inhibition, we interrogated our RNA-sequencing dataset, and identified differences between HBVPs, mesoderm and neural crest iPericytes, in the relative expression of mRNAs downstream of the PDGF-BB:PDGFR β pathway. In particular, *PIK3CA* (log2FoldChange = -0.67, $p_{\text{adj}} = 2.76E^{-5}$), *NFKB1* (log2FoldChange = -1.28, $p_{\text{adj}} = 2.47E^{-26}$), *NFKB2* (log2FoldChange = -0.78, $p_{\text{adj}} = 0.00096$), *CREB1* (log2FoldChange = -0.46, $p_{\text{adj}} = 2.39E^{-6}$) and *PTPN11* (log2FoldChange = -0.36, $p_{\text{adj}} = 0.003$) were differentially expressed between HBVPs and iPericytes, while *PIK3CA* (log2FoldChange = -0.44, $p_{\text{adj}} = 0.039$) and *NFKB2* (log2FoldChange = 0.68, $p_{\text{adj}} = 2.24E^{-5}$) were differentially expressed between mesoderm and neural crest iPericytes (Fig. 4D). RNAseq analysis also revealed that the

expression of *PDGFR β* was significantly higher (log2FoldChange = -1.06, $p_{\text{adj}} = 6.26E^{-6}$) in neural crest iPericytes compared to mesoderm iPericytes (Fig. 4D), which is in line with the qPCR data (Fig. 1B). These differences could explain why neural crest iPericytes required a higher concentration of imatinib to prevent PDGF-BB mediated proliferation.

iPericytes contract in response to endothelin-1

A primary function of pericytes is to contract and dilate to modulate capillary diameter, thereby altering cerebral blood flow [4]. We previously used a single cell imaging assay [24] and the xCelligence electrical impedance assay [23] to show that HBVPs can respond to vasoactive mediators. To assess the responses of mesoderm and neural crest iPericytes to endothelin-1, we again used the xCelligence system. Cells were plated on specialised cell culture plates that allow resistance to electron flow to be measured to provide an assessment of cell index (Additional file 1: Fig. S6A). Normalised cell index values can be analysed to compare differences in slope, AUC and change in cell area after treatment with contractile mediators (Additional file 1: Fig. S6B). It is important to note that a small reduction in normalised cell index is ordinarily observed over the first few minutes of an experiment, even under control conditions (Fig. 5A, B, [23]). When mesoderm iPericytes (Fig. 5A) and neural crest iPericytes (Fig. 5B) were treated with endothelin-1, normalised cell index decreased compared to vehicle suggesting pericytes had contracted, which was confirmed when AUC was calculated (treatment: $p=0.0033$, Fig. 5C; treatment: $p<0.0001$, Fig. 5F). Compared to HBVPs, contraction of mesoderm iPericytes ($p=0.9995$, Fig. 5C) and neural crest iPericytes ($p=0.1464$, Fig. 5F) was similar in the first 20 min of endothelin-1 exposure. The maximum contraction achieved by mesoderm iPericytes was the same as HBVPs in response to endothelin-1 (treatment: $p=0.0021$, Fig. 5D), and this was maintained over

(See figure on next page.)

Fig. 4 Proliferation of iPericytes through the PDGF-BB: PDGFR β signalling pathway. **A** iPericytes were incubated in basal pericyte media (PM) and treated with PDGF-BB (PM + PDGF-BB) while being exposed to 100 μ M imatinib (PM + PDGF-BB + 100 μ M imatinib). Proliferation was measured using an EdU uptake assay. iPericytes that are EdU-positive are indicated by magenta, while total number of iPericytes were measured by DAPI (blue). Scale bar = 50 μ m. **B** Quantification of HBVPs, neural crest iPericytes and mesoderm iPericytes proliferating (as indicated by EdU-positive staining) as a percentage of total cells following 24 h exposure to PM, complete pericyte media with pericyte growth factors (CPM) or PM + PDGF-BB ($n=8$ per condition). Data were analysed using a one-way ANOVA: HBVP ($F(2, 21) = 35.52, p<0.0001$); neural crest iPericyte ($F(2, 21) = 30.85, p<0.0001$); mesoderm iPericyte ($F(2, 21) = 191.4, p<0.0001$). **C** Quantification of changes to PDGF-BB-induced proliferation with increasing concentrations of imatinib over 24 h in HBVPs, neural crest iPericytes and mesoderm iPericytes ($n=8$ per condition). Data were analysed using a one-way ANOVA or Kruskal–Wallis test: HBVP ($F(3, 26) = 259.2, p<0.0001$); neural crest iPericyte ($H(3) = 24.41, p<0.0001$); mesoderm iPericyte ($F(3, 28) = 221.5, p<0.0001$). For **B, C**, post-hoc comparisons were performed using Dunnett's multiple comparisons or Dunn's test: * $p<0.05$; ** $p<0.01$; *** $p<0.001$; **** $p<0.0001$. Data shown as mean \pm SD. **D** Heat map of key genes involved in pericyte proliferation in the PDGF-BB: PDGFR β signalling pathway in HBVP, neural crest iPericytes and mesoderm iPericytes selected from Sweeney et al. [29]

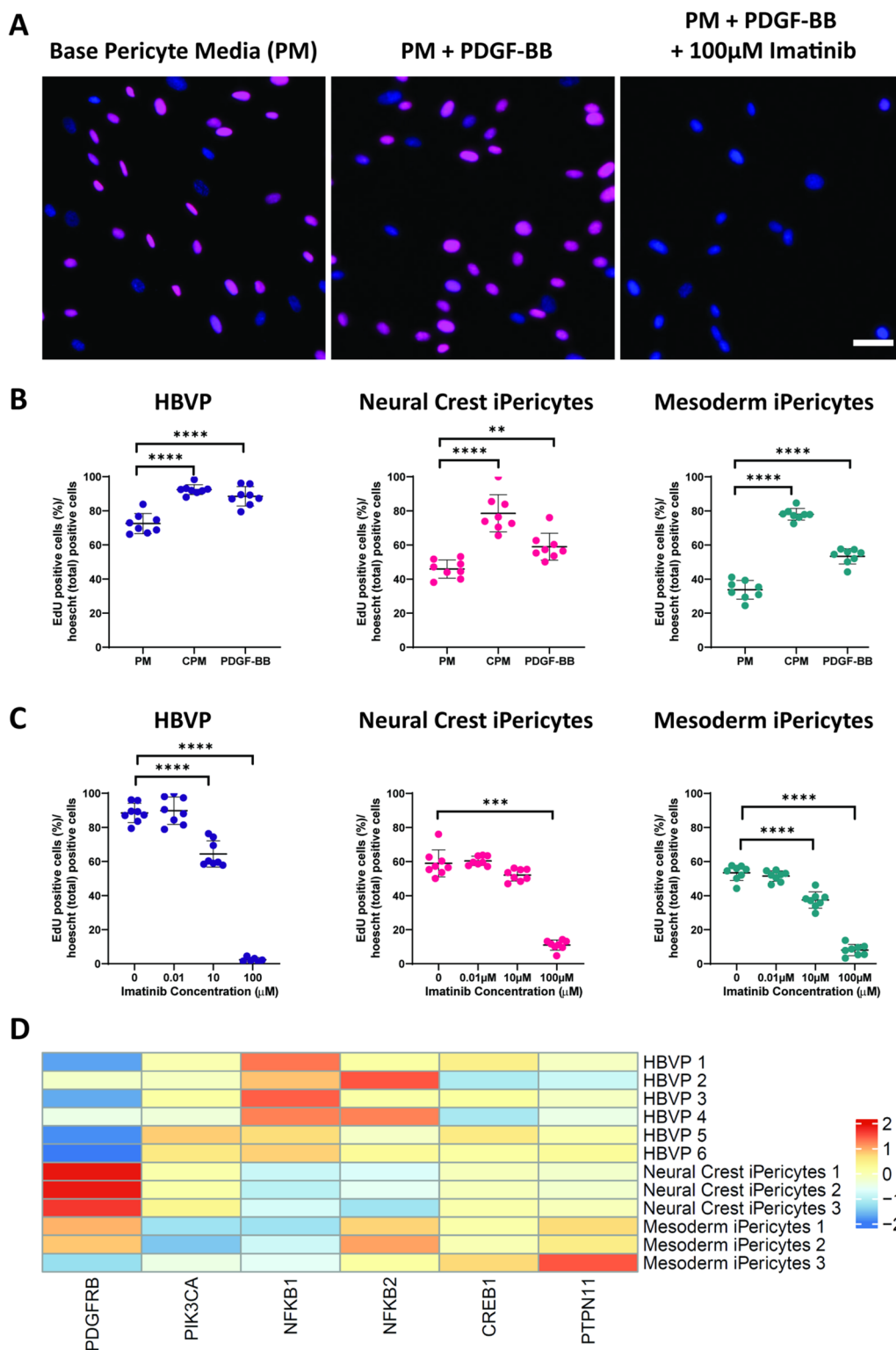


Fig. 4 (See legend on previous page.)

2 h (treatment: $p=0.0026$, Fig. 5E). However, there was a different effect of treatment with endothelin-1 on neural crest iPericytes in comparison to HBVPs (interaction of cell type \times treatment: $p=0.0010$, Fig. 5G). Post-hoc analysis revealed that neural crest iPericytes maximum contraction was greater in response to endothelin-1 compared to HBVPs ($p=0.0007$, Fig. 5G) and they also sustained a greater level of contraction compared to HBVPs for up to 2 h ($p=0.0001$, Fig. 5H). These findings suggest that iPericytes derived through different lineages display distinct responses to endothelin-1.

To determine whether the lineage specific responses of iPericytes were due to differences in endothelin-1 receptor expression, we determined whether endothelin-1 receptor genes were differentially expressed between HBVPs, neural crest iPericytes and mesoderm iPericytes. *EDNRA* and *EDNRB*, genes which code for the two major endothelin-1 receptors, were differentially expressed in our RNA-seq dataset. There was a significantly different expression of both subtypes of endothelin-1 receptor between HBVPs and neural crest iPericytes (*EDNRA*: Fig. 5I, $\log_2\text{FoldChange}=2.53$, $p_{\text{adj}}=6.12E^{-23}$; *EDNRB*: Fig. 5J $\log_2\text{FoldChange}=5.14$, $p_{\text{adj}}=9.13E^{-26}$), while there was no difference between HBVP and mesoderm iPericytes (Fig. 5I, J). There was also significantly higher expression of both subtypes of endothelin-1 receptor in neural crest iPericytes compared to mesoderm iPericytes (*EDNRA*: Fig. 5I, $\log_2\text{FoldChange}=-2.52$, $p_{\text{adj}}=3.12E^{-25}$; *EDNRB*: Fig. 5J, $\log_2\text{FoldChange}=-7.22$, $p_{\text{adj}}=6.77E^{-15}$), which might be driving their greater response to the endothelin-1 ligand. These data indicate that iPericytes can respond to endothelin-1, and that neural crest iPericytes display a greater contractile response to endothelin-1 compared to mesoderm iPericytes and HBVPs.

iPericytes have functional responses to the vasodilator adenosine

Given we observed differences in the response of neural crest iPericytes and mesoderm iPericytes to endothelin-1, we also tested the response of iPericytes to adenosine which can initiate pericyte relaxation in vitro [23]. Similar to HBVPs, when mesoderm iPericytes (Fig. 6A) and neural crest iPericytes (Fig. 6B) were exposed to adenosine, normalised cell index increased compared to vehicle conditions, indicative of pericyte relaxation. When treated with adenosine, mesoderm iPericytes relaxed (treatment: $p=0.0002$, Fig. 6C) and the maximum relaxation achieved by mesoderm pericytes was the same as HBVPs in response to adenosine (treatment: $p=0.0002$, Fig. 6D), however, this was not maintained over 2 h (treatment: $p=0.7317$, Fig. 6E). There was a different response following adenosine treatment on neural crest iPericyte relaxation in comparison to HBVPs (interaction of cell type \times treatment: $p=0.0202$, Fig. 6F). Post-hoc analysis revealed that neural crest iPericytes relax less in response to adenosine compared to HBVPs ($p=0.0112$, Fig. 6F), which was also observed in assessment of maximum relaxation ($p=0.0336$, Fig. 6G) and relaxation at 2 h ($p=0.0170$, Fig. 6H). These findings indicate that neural crest iPericytes display reduced ability to relax in response to adenosine compared to mesoderm iPericytes.

To determine whether the lineage specific responses of iPericytes were due to differences in adenosine receptor expression, we determined whether adenosine receptor genes were differentially expressed between HBVPs, neural crest iPericytes and mesoderm iPericytes. *ADORA1* and *ADORA2B*, genes which code for two of the major adenosine receptors, were differentially expressed in our RNA-seq dataset. There was a significantly different

(See figure on next page.)

Fig. 5 Endothelin-1 induces iPericyte contraction. **A, B** Normalised cell index of neural crest iPericytes, mesoderm iPericytes and HBVPs treated with endothelin-1 or vehicle (CPM) over a period of 2 h ($n=4$ per condition). **C–E** Quantified AUC (**C**; indicator of volume of contraction), Δ cell index (**D**; maximum contraction) and Δ cell index after 2 h (**E**; contraction at 2 h time point) for mesoderm iPericytes and HBVPs treated with control or endothelin-1 analysed using two-way ANOVA: AUC (cell type: $F(1, 12)=0.6953$, $p=0.4206$; treatment: $F(1, 12)=13.35$, $p=0.0033$; interaction: $F(1, 12)=0.1006$, $p=0.7565$); Δ cell index (cell type: $F(1, 12)=0.02309$, $p=0.8817$; treatment: $F(1, 12)=15.21$, $p=0.0021$; interaction: $F(1, 12)=0.5773$, $p=0.4620$); Δ cell index after 2 h (cell type: $F(1, 12)=1.590$, $p=0.2313$; treatment: $F(1, 12)=14.31$, $p=0.0026$; interaction: $F(1, 12)=0.5518$, $p=0.4719$). **F–H** Quantified AUC (**F**), Δ cell index (**G**) and Δ cell index after 2 h (**H**) for neural crest iPericytes and HBVPs treated with control or endothelin-1 analysed using two-way ANOVA: AUC (cell type: $F(1, 12)=1.563$, $p=0.2351$; treatment: $F(1, 12)=54.67$, $p<0.0001$; interaction: $F(1, 12)=5.470$, $p=0.0375$); Δ cell index (cell type: $F(1, 12)=13.53$, $p=0.0032$; treatment: $F(1, 12)=66.11$, $p<0.0001$; interaction: $F(1, 12)=18.47$, $p=0.0010$); Δ cell index after 2 h (cell type: $F(1, 12)=34.64$, $p<0.0001$; treatment: $F(1, 12)=38.56$, $p<0.0001$; interaction: $F(1, 12)=14.70$, $p=0.0024$). **C–H** Post-hoc comparisons performed using Sidak's multiple comparisons test. * $p<0.05$; ** $p<0.01$; *** $p<0.001$; **** $p<0.0001$. Data shown as mean \pm SD. **I–J** Normalised gene expression counts of differentially expressed endothelin-1 receptors in HBVP, neural crest iPericytes and mesoderm iPericytes compared using DEseq: HBVPs and neural crest iPericytes *EDNRA*, **I** $\log_2\text{FoldChange}=2.53$, $p_{\text{adj}}=6.12E^{-23}$, *EDNRB*, **J** $\log_2\text{FoldChange}=5.14$, $p_{\text{adj}}=9.13E^{-26}$, neural crest iPericytes compared to mesoderm iPericytes *EDNRA*, **I** $\log_2\text{FoldChange}=-2.52$, $p_{\text{adj}}=3.12387E^{-25}$, *EDNRB*, **J** $\log_2\text{FoldChange}=-7.22$, $p_{\text{adj}}=6.77016E^{-15}$

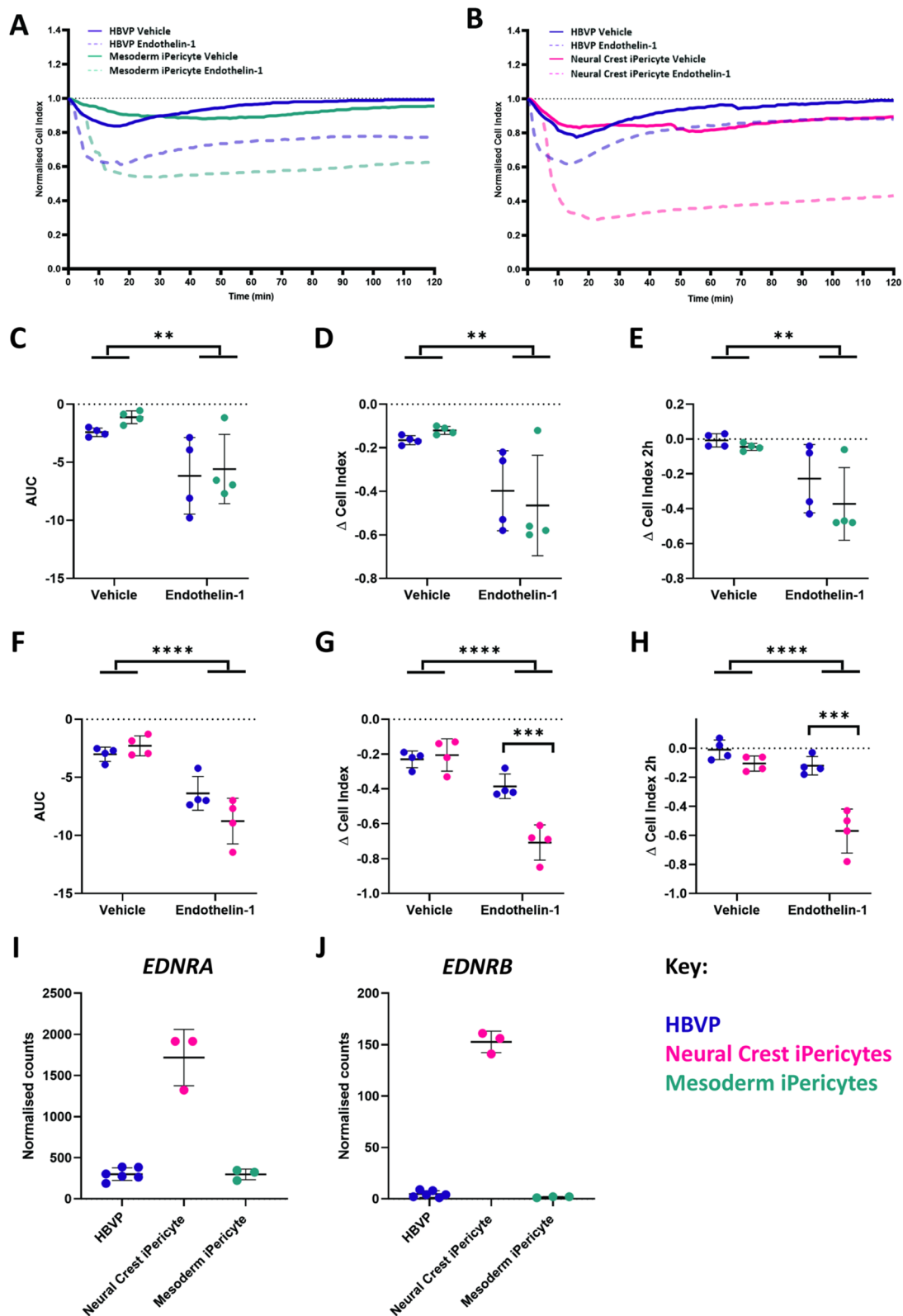


Fig. 5 (See legend on previous page.)

expression of adenosine receptors type *ADORA1* and *ADORA2B* between HBVPs and neural crest iPericytes (*ADORA1*: Fig. 6I, $\log_2\text{FoldChange} = 3.92$, $p_{\text{adj}} = 1.65E^{-11}$; *ADORA2B*: Fig. 6J, $\log_2\text{FoldChange} = -1.71$, $p_{\text{adj}} = 2.93E^{-19}$). There was also significantly higher expression of both of these subtypes in neural crest iPericytes compared to mesoderm iPericytes (*ADORA1*: Fig. 6I, $\log_2\text{FoldChange} = -1.19$, $p_{\text{adj}} = 0.001$; *ADORA2B*: Fig. 6J, $\log_2\text{FoldChange} = -0.61$, $p_{\text{adj}} = 0.033$). Therefore, while differences in the expression of adenosine receptors exist between HBVPs, mesoderm and neural crest iPericytes, they do not reflect differences in functional responses to adenosine. These findings suggest that iPericytes can respond to adenosine, and that neural crest iPericytes display a reduced relaxation response compared to HBVPs.

Discussion

iPSC-derived neurovascular cells are becoming a popular model of choice to investigate the function of the NVU in vitro. Methods to generate iPericytes reveal a novel avenue that will allow researchers to determine how patient specific genetic variants affect pericyte function, will help to create more accurate in vitro models of the NVU and disease and, ultimately, may provide a reproducible and personalised tool for implantation in regenerative medicine. To confidently use these cells to study pericyte function, it is important to establish how representative they are of primary pericytes in vitro. We derived mesoderm and neural crest iPericytes using a previously published protocol [17] and showed they express classical pericyte mRNAs, but do not express other brain cell markers. We then found that there were differences between mesoderm and neural crest iPericytes in their functional response to the PDGF-BB:PDGFR β signalling pathway that mediates proliferation, and in response to

known vasoactive mediators endothelin-1 and adenosine, in comparison to HBVPs.

Mesoderm and neural crest iPericytes express key pericyte markers and morphologies

Using both qPCR and immunocytochemistry, we sought to test the expression of key pericyte mRNAs or proteins in neural crest and mesoderm iPericytes derived from the TOB-00220 line. We found that both developmental lineages of iPericytes express three classical pericyte mRNAs *ANPEP* (encoding CD13), *CSPG4* (encoding NG2) and *PDGFRB* (encoding PDGFR β), with immunocytochemistry confirming their protein expression, in line with a previous study [17]. Importantly, we also compared iPericyte mRNAs expression to primary HBVPs and showed high levels of expression compared to iPSCs. iPericytes downregulate expression of key pluripotency mRNAs *OCT4* and *NANOG*, showing a distinct change compared to the iPSCs from which they were derived. In addition, iPericytes display the five morphological subtypes previously described for primary HBVPs [24]. The majority of cells exhibited standard morphology, which we have previously shown possess contractile capacity [24]. These data highlight that iPericytes express pericyte markers and are morphologically similar to HBVPs.

iPericytes retain lineage specific differences in gene expression

We next sought to understand whether separate iPericyte lineages could display altered gene expression and which biological processes these were related to. Following RNA sequencing, we showed that gene expression in HBVPs was markedly different compared to both mesoderm and neural crest iPericytes. Differentially expressed genes appeared to be related to tissue development and protein binding, which could impact the function of these cells. It

(See figure on next page.)

Fig. 6 Adenosine induces iPericyte relaxation. **A, B** Normalised cell index of neural crest iPericytes, mesoderm iPericytes and HBVPs treated with adenosine or vehicle (CPM) over a period of 2 h ($n=4$ per condition). **C–E** Quantified AUC (C), Δ cell index (D) and Δ cell index after 2 h (E) for mesoderm iPericytes and HBVPs treated with control or adenosine analysed using two-way ANOVA: AUC (cell type: $F(1, 12) = 6.583$, $p = 0.0247$; treatment: $F(1, 12) = 26.84$, $p = 0.0002$; interaction: $F(1, 12) = 6.027$, $p = 0.0303$); Δ cell index (cell type: $F(1, 12) = 6.387$, $p = 0.0265$; treatment: $F(1, 12) = 28.26$, $p = 0.0002$; interaction: $F(1, 12) = 1.284$, $p = 0.2794$); Δ cell index after 2 h (cell type: $F(1, 12) = 1.460$, $p = 0.2502$; treatment: $F(1, 12) = 0.1232$, $p = 0.7317$; interaction: $F(1, 12) = 1.174$, $p = 0.2999$). **F–H** Quantified AUC (F), Δ cell index (G) and Δ cell index after 2 h (H) for neural crest iPericytes and HBVPs treated with control or adenosine analysed using two-way ANOVA: AUC (cell type: $F(1, 12) = 8.596$, $p = 0.0126$; treatment: $F(1, 12) = 50.38$, $p < 0.0001$; interaction: $F(1, 12) = 7.159$, $p = 0.0202$); Δ cell index (cell type: $F(1, 12) = 7.881$, $p = 0.0158$; treatment: $F(1, 12) = 57.12$, $p < 0.0001$; interaction: $F(1, 12) = 3.777$, $p = 0.0758$); Δ cell index after 2 h (cell type: $F(1, 12) = 16.46$, $p = 0.0016$; treatment: $F(1, 12) = 20.58$, $p = 0.0007$; interaction: $F(1, 12) = 1.500$, $p = 0.2442$). **C–H** Post-hoc comparisons performed using Sidak's multiple comparisons test. * $p < 0.05$; ** $p < 0.01$; *** $p < 0.001$; **** $p < 0.0001$. Data shown as mean \pm SD. **I, J** Normalised gene expression counts of differentially expressed adenosine receptors in HBVP, neural crest iPericytes and mesoderm iPericytes compared using DEseq: HBVPs and neural crest iPericytes *ADORA1*, **I** $\log_2\text{FoldChange} = 3.92$, $p_{\text{adj}} = 1.65E^{-11}$; *ADORA2B*, **J** $\log_2\text{FoldChange} = -1.71$, $p_{\text{adj}} = 2.93E^{-19}$; HBVPs and mesoderm iPericytes *ADORA1*, **I** $\log_2\text{FoldChange} = 2.72$, $p_{\text{adj}} = 0.00006$; *ADORA2B*, **J** $\log_2\text{FoldChange} = -2.33$, $p_{\text{adj}} = 1.52E^{-25}$; neural crest iPericytes compared to mesoderm iPericytes *ADORA1*, **I** $\log_2\text{FoldChange} = -1.19$, $p_{\text{adj}} = 0.001$; *ADORA2B*, **J** $\log_2\text{FoldChange} = -0.61$, $p_{\text{adj}} = 0.03288$

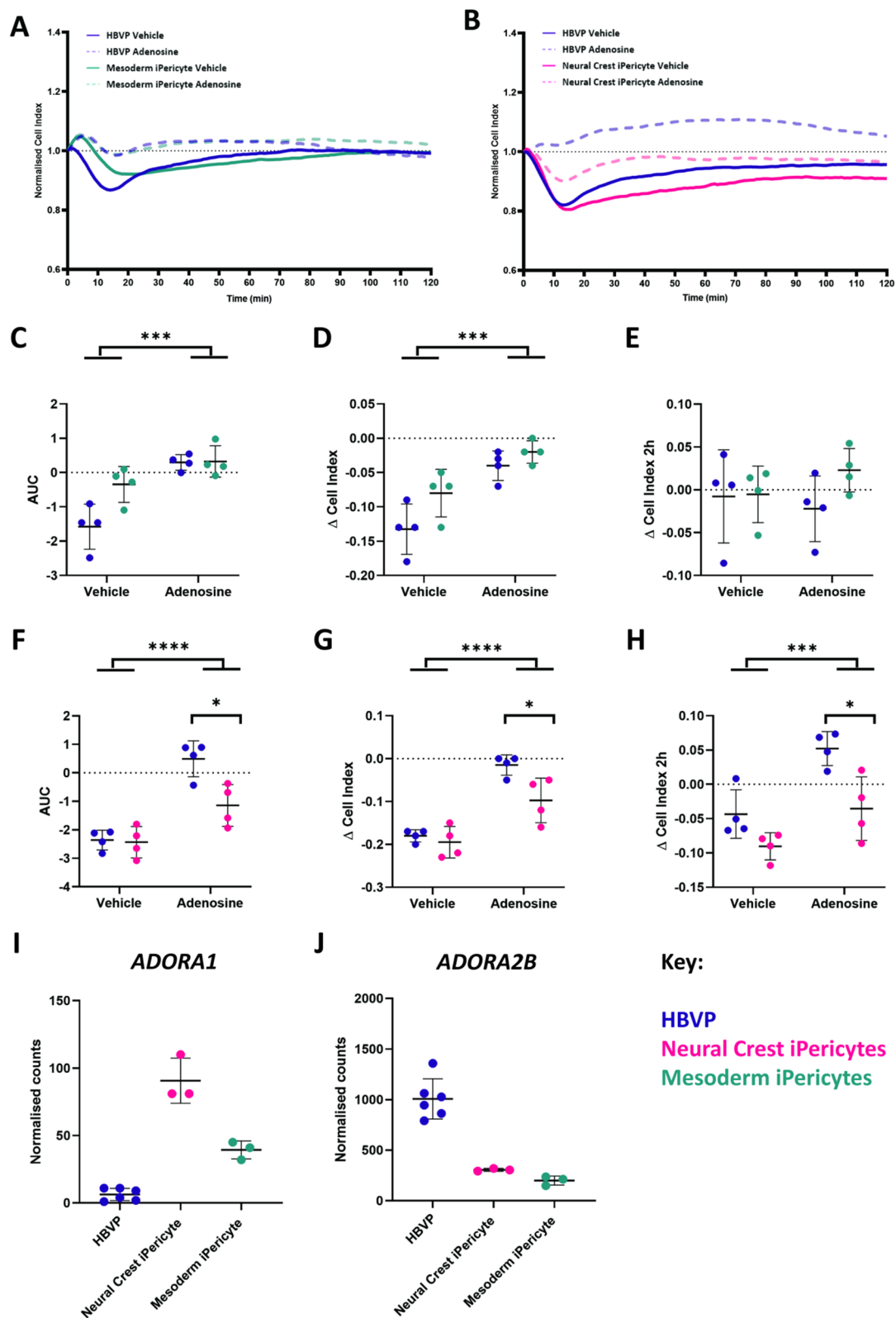


Fig. 6 (See legend on previous page.)

has already been shown that pericytes contribute to the development of the vascular network in multiple organs and they can assist in the development of key cellular structures such as the extracellular matrix [26]. It is possible that differences in the genetic background of HBVPs compared to the iPSC line we used for differentiation to neural crest and mesoderm iPericytes could explain the extent of differential gene expression. In addition, HBVPs could include both mesoderm and neural crest-derived pericytes given that both lineages reside in the brain [7]. Another possibility is that iPericytes could be a more immature population of cells compared to HBVPs, driving similarities between iPericyte lineages in comparison to HBVPs. However, it is important to note that the developmental stage of HBVPs is unknown, and therefore it is difficult to make conclusions about the developmental state of iPericytes compared to HBVPs [27]. We also identified that there were gene expression differences between neural crest and mesoderm iPericytes that was related primarily to organ development. These differences could be explained by the mesoderm lineage being more prominent in organ development throughout the body whereas cells from the neural crest pathway would be restricted to the nervous system [28]. Interestingly, genes related to growth factor binding and activity were also differentially expressed which could indicate differences in function of pericytes derived from these two lineages. This was evident in both the proliferation and contractility assays where functional responses differed, suggesting pericytes of different lineages may have altered physiological responses.

iPericytes can be consistently produced from different iPSC lines

Using RNA sequencing, we showed that gene expression profiles of iPericytes that had been differentiated from three separate iPSC lines derived from three unrelated individuals were consistent between different lines. In particular, all three iPericyte lines had consistent levels of enriched pericyte mRNA expression, while down-regulating expression of known stem cell genes. Notably, iPericytes did not express key markers of any other cell type such as endothelial cells, microglia, OPCs, oligodendrocytes, astrocytes, or neurons. This suggests that iPericytes can be produced with high consistency from different iPSC lines, supporting their use for assessing pericyte function in disease contexts.

iPericytes proliferate in response to the PDGFR β ligand PDGF-BB

Although consistent expression of key pericyte mRNAs and proteins by iPericytes is encouraging, it is important that this translates into functional characteristics

representative of pericytes in vivo. To expand our knowledge on the relative similarities between mesoderm and neural crest iPericytes, we compared their functional response to PDGF-BB, a growth factor essential for pericyte proliferation and survival [29]. We have previously shown that HBVPs proliferate in response to PDGF-BB in vitro through the PDGFR β receptor [21]. Like HBVPs, mesoderm and neural crest iPericytes proliferated in the presence of PDGF-BB. In addition, the specificity of this proliferative response to the PDGFR β pathway was confirmed by the blockade of this response with the PDGFR β inhibitor imatinib, similar to HBVPs. The PDGF-BB:PDGFR β signalling pathway is essential for pericyte and endothelial cell interactions at the NVU, mediating key endothelial cell processes such as angiogenesis [29]. A number of studies have assessed iPericytes in co-culture with endothelial cells [8–10, 15], showing that iPericytes can specifically support endothelial tube formation and the strength of the endothelial barrier through trans-endothelial resistance measures [7–10, 17]. In addition, iPericytes have been used as part of functional blood–brain barrier models [7, 30–32]. Furthermore, a recent study showed the capacity of iPericytes to aid in BBB repair in pericyte deficient mice, suggesting functional signalling between endothelial cells and iPericytes is also possible in vivo [33]. These studies highlight the capacity for iPericytes to support and enhance survival and differentiation of other key cells of the NVU. Future studies could characterise differences between mesoderm and neural crest iPericyte interactions with endothelial cells or other NVU cell types using co-culture methods, as there may be differences between pericyte lineages in the ability to support these functions.

Until now functional studies of iPericytes have typically focussed on one pericyte developmental lineage at a time, either mesoderm [8–10] or neural crest [7, 11], restricting comparisons between the two. Here, we demonstrate for the first time that neural crest iPericytes display altered PDGFR β signalling responses compared to HBVPs and mesoderm iPericytes, with a higher concentration of the PDGFR β receptor inhibitor imatinib required to inhibit proliferation in vitro. This finding was supported by higher expression of the *PDGFRB* gene by neural crest iPericytes. These differences may reflect an inherent difference in the function of this receptor pathway between neural crest and mesoderm pericytes that should be considered for future studies.

iPericytes are responsive to the vasoactive mediators endothelin-1 and adenosine

Another key function of pericytes is their role in blood flow regulation. It has previously been shown that pericytes possess the contractile protein α SMA which can

generate a contractile response in these cells [34, 35]. However, there has been some discordance in the literature about expression of α SMA and contractility of pericytes [4, 36]. This discordance has also been observed with iPericytes in vitro with some studies showing α SMA expression in iPericytes [10, 11] and some concluding that it is not expressed [7, 8]. Interestingly, Kumar et al. [10] found that α SMA expression could be triggered through a specific pericyte differentiation protocol involving PDGF-BB, vascular endothelial growth factor (VEGF), activin receptor-like kinase receptor (ALK) inhibitor SB-431542 and epidermal growth factor (EGF), suggesting certain growth factors must be present for expression of α SMA in iPericytes. Here, we showed that the α SMA gene *ACTA2* was expressed in both neural crest and mesoderm iPericytes, with bulk RNA sequencing revealing reproducible expression of *ACTA2* in mesoderm iPericytes throughout three separate iPSC lines. Given that HBVP expression of α SMA was associated with contractile ability [24], the expression of α SMA is suggestive of the potential to contract.

It has previously been shown that HBVPs contract in response to endothelin-1 and relax in response to adenosine in vitro [23]. Using a similar approach, we found that exposing neural crest and mesoderm iPericytes to endothelin-1 led to a strong reduction in cell area indicative of cell contraction. Interestingly, neural crest iPericytes had a much stronger contractile response to endothelin-1 compared to both HBVPs and mesoderm iPericytes. Further analysis into gene expression changes revealed that the two major endothelin-1 receptors (*EDNRA* and *EDNRB*) were more highly expressed in neural crest iPericytes. In addition, the expression of *ACTA2*, the gene encoding the key contractile protein α SMA, was more highly expressed by neural crest iPericytes. However, neural crest iPericytes appear to not relax in response to adenosine as much as HBVPs and mesoderm iPericytes. Given that neural crest iPericytes expressed similar (*ADORA2B*) or higher (*ADORA1*) levels of adenosine receptor compared to mesoderm iPericytes, this suggests other factors may be influencing the extent to which neural crest iPericytes react to adenosine. Overall, these experiments highlight the ability of iPericytes to contract and relax, with mesoderm iPericytes displaying the most similar functional contractile responses to HBVPs.

Both mesoderm and neural crest iPericytes can be used for in vitro studies of pericyte function

With the recent discoveries of the multiple functions pericytes play [37], iPSC derived pericytes are becoming a popular model of choice for in vitro studies, particularly to understand functional changes and impact of genetic

variants [7, 17]. This study highlights the similarities and differences between iPericytes derived through two developmental lineages: neural crest and mesoderm. It is difficult to recommend a specific lineage of pericytes as more relevant for cell culture studies as human brain pericytes arise from both the mesoderm and neural crest lineage [17]. In addition, there is lineage specific localisation of pericytes with neural crest pericytes present in the forebrain, whereas mesoderm pericytes are present in the brainstem, mid-brain and spinal cord [17, 38]. However, it is currently unclear whether mixed populations occur within the same region of the brain. For example, using *PUI-/-* mice to knockout the myeloid lineage (mesoderm origin), pericyte number in the midbrain was reduced but not completely absent, suggesting contributions from other lineages such as neural crest [39]. In our hands, while there were morphological and gene expression similarities between HBVPs and both iPericyte lineages, it appeared that mesoderm iPericytes resembled HBVPs more closely in a functional capacity. Therefore, both neural crest and mesoderm iPericytes appear to be appropriate to model brain pericytes for the study of pericyte biology.

Conclusion

Collectively, we illustrate that neural crest and mesoderm iPericytes, derived from multiple iPSC lines, are morphologically similar to HBVPs and express key pericyte markers. iPericytes are functionally active, demonstrated through proliferation in response to the key pericyte growth factor PDGF-BB, contraction in response to endothelin-1, and relaxation in response to adenosine. These findings suggest that iPericytes behave functionally like HBVPs, providing further support for their use as a tool to study pericyte function. We observed some differences between iPericytes of different lineages, notably that neural crest iPericytes were less sensitive to PDGFR β inhibition and more contractile compared to mesoderm iPericytes and HBVPs. Therefore, mesoderm iPericytes are functionally the most similar to HBVPs in vitro and differences between iPericytes derived through different lineages must be taken into consideration when designing experiments using iPericytes to assess pericyte function.

Supplementary Information

The online version contains supplementary material available at <https://doi.org/10.1186/s13287-024-03671-x>.

Additional file 1: Supplementary methods and figures.

Acknowledgements

We would like to thank study participants who donated cells for iPSC generation. The University of Tasmania provided core laboratory facilities for this

work. We would like to acknowledge the use of the high-performance computing facilities provided by Digital Research at the University of Tasmania. We would like to acknowledge the Australian Genome Research Facility (AGRF) who performed all of the RNA sequencing for gene expression analysis.

Author contributions

NEK: methodology; validation; investigation; formal analysis; visualisation; writing—original draft; writing—review and editing. J-MC: methodology; software; formal analysis; investigation; resources; data curation; writing—review and editing; visualisation; supervision. LSB: methodology; formal analysis; investigation; writing—review and editing; visualisation. AJF: investigation; methodology; formal analysis; visualisation; writing—review and editing. NBB: data curation; methodology; formal analysis; visualisation; supervision; writing—review and editing. JLF: investigation; methodology; supervision; writing—review and editing. JMC: methodology; investigation; writing—review and editing. JT: methodology; writing—review and editing. AP: methodology; resources; writing—review and editing. AWH: methodology; resources; writing—review and editing. GPM: methodology; supervision; writing—original draft; writing—review and editing. KMY: conceptualisation; funding acquisition; methodology; project administration; resources; supervision; writing—review and editing. ALC: conceptualisation; funding acquisition; methodology; project administration; resources; supervision; writing—review and editing. BAS: conceptualisation; funding acquisition; methodology; project administration; resources; supervision; writing—original draft; writing—review and editing.

Funding

This project was supported by funding from the University of Tasmania College of Health and Medicine Research Enhancement Program, National Health and Medical Research Council (APP1137776 and APP1163384), Medical Research Future Fund (EPCD000008), MS Australia (19-0696, 20-137, 21-3-023, 22-4-097), the Menzies Institute for Medical Research, and the Irene Phelps Charitable Trust. NEK, LSB and JMC were supported by Tasmanian Graduate Research Scholarships. AJF was supported by a Research Training Program Scholarship.

Availability of data and materials

RNA sequencing data from HBVPs and iPercytes differentiated from the TOB-00220 iPSC line have been deposited in NCBI's Gene Expression Omnibus [40] and are accessible through GEO Series accession number GSE252046 (<https://www.ncbi.nlm.nih.gov/geo/query/acc.cgi?acc=GSE252046>). RNA sequencing data from iPSC lines MNZTASi019-A, MNZTASi021-A and MNZTASi022-A have been deposited in the European Genome Phenome Archive (EGAD50000000255, <https://ega-archive.org/datasets/EGAD50000000255>). iPSC lines MNZTASi019-A, MNZTASi021-A and MNZTASi022-A can be obtained from the MS Stem biobank (<https://msresearchflagship.org.au/researchers/ms-stem>). All other data are available from the corresponding author upon reasonable request.

Declarations

Ethics approval and consent to participate

The TOB-00220 iPSC line was cultured under the project "Use of induced pluripotent stem cell lines from repositories, commercial sources, and academic collaborators" approved by the University of Tasmania Human Research Ethics Committee (Project Number H26563 approved on 23rd November 2021). MNZTASi019-A, MNZTASi021-A and MNZTASi022-A, were purchased from the MS Stem biobank (Menzies Institute for Medical Research, Hobart, Tasmania, Australia) and had been previously generated under the project "Investigating molecular mechanisms of Multiple Sclerosis in induced pluripotent stem cells" approved by the University of Tasmania Human Research Ethics Committee (Project Number H16915 approved on 12th December 2017).

Consent for publication

All participants provided consent for participation in the research and publication of the resulting data.

Competing interests

The authors declare that they have no competing interests.

Author details

¹Tasmanian School of Medicine, College of Health and Medicine, University of Tasmania, Level 4, Medical Sciences Precinct, 17 Liverpool St, Hobart, TAS 7000, Australia. ²Menzies Institute for Medical Research, University of Tasmania, Hobart, Australia. ³Wicking Dementia Education and Research Centre, College of Health and Medicine, University of Tasmania, Hobart, Australia. ⁴Department of Anatomy and Physiology, The University of Melbourne, Melbourne, Australia. ⁵Department of Surgery, Royal Melbourne Hospital, The University of Melbourne, Melbourne, Australia. ⁶Centre for Eye Research Australia, Royal Victorian Eye and Ear Hospital, East Melbourne, Australia.

Received: 18 October 2023 Accepted: 16 February 2024

Published online: 03 March 2024

References

- Brown LS, Foster CG, Courtney J-M, King NE, Howells DW, Sutherland BA. Pericytes and neurovascular function in the healthy and diseased brain. *Front Cell Neurosci.* 2019;13:282.
- Cashion JM, Young KM, Sutherland BA. How does neurovascular unit dysfunction contribute to multiple sclerosis? *Neurobiol Dis.* 2023;178:106028.
- Nortley R, Korte N, Izquierdo P, Hirunpattarasilp C, Mishra A, Jaunmuktane Z, et al. Amyloid beta oligomers constrict human capillaries in Alzheimer's disease via signaling to pericytes. *Science.* 2019;365:6450.
- Hall CN, Reynell C, Gesslein B, Hamilton NB, Mishra A, Sutherland BA, et al. Capillary pericytes regulate cerebral blood flow in health and disease. *Nature.* 2014;508(7494):55–60.
- Shibahara T, Ago T, Nakamura K, Tachibana M, Yoshikawa Y, Komori M, et al. Pericyte-mediated tissue repair through PDGFR β promotes perinfarct astrogliosis, oligodendrogenesis, and functional recovery after acute ischemic stroke. *eNeuro.* 2020;7(2).
- Kusuma S, Shen YI, Hanjaya-Putra D, Mali P, Cheng L, Gerecht S. Self-organized vascular networks from human pluripotent stem cells in a synthetic matrix. *Proc Natl Acad Sci U S A.* 2013;110(31):12601–6.
- Stebbins MJ, Gastfriend BD, Canfield SG, Lee MS, Richards D, Faubion MG, et al. Human pluripotent stem cell-derived brain pericyte-like cells induce blood-brain barrier properties. *Sci Adv.* 2019;5(3):7375.
- Dar A, Domev H, Ben-Yosef O, Tzukerman M, Zeevi-Levin N, Novak A, et al. Multipotent vasculogenic pericytes from human pluripotent stem cells promote recovery of murine ischemic limb. *Circulation.* 2012;125(1):87–99.
- Orlova VV, Drabsch Y, Freund C, Petrus-Reurer S, van den Hil FE, Muenthai-song S, et al. Functionality of endothelial cells and pericytes from human pluripotent stem cells demonstrated in cultured vascular plexus and zebrafish xenografts. *Arterioscler Thromb Vasc Biol.* 2014;34(1):177–86.
- Kumar A, D'Souza SS, Moskvina OV, Toh H, Wang B, Zhang J, et al. Specification and diversification of pericytes and smooth muscle cells from mesenchymal angioblasts. *Cell Rep.* 2017;19(9):1902–16.
- Kelleher J, Dickinson A, Cain S, Hu Y, Bates N, Harvey A, et al. Patient-specific iPSC model of a genetic vascular dementia syndrome reveals failure of mural cells to stabilize capillary structures. *Stem Cell Rep.* 2019;13(5):817–31.
- Fortune AJ, Fletcher JL, Blackburn NB, Young KM. Using MS induced pluripotent stem cells to investigate MS aetiology. *Mult Scler Relat Disord.* 2022;63:103839.
- Stanton AE, Bubnys A, Agbas E, James B, Park DS, Jiang A, et al. Engineered 3D immuno-glia-neurovascular human brain model. *bioRxiv.* 2023.
- Tachibana M, Yamazaki Y, Liu CC, Bu G, Kanekiyo T. Pericyte implantation in the brain enhances cerebral blood flow and reduces amyloid- β pathology in amyloid model mice. *Exp Neurol.* 2018;300:13–21.
- Orlova VV, van den Hil FE, Petrus-Reurer S, Drabsch Y, Ten Dijke P, Mummery CL. Generation, expansion and functional analysis of endothelial cells and pericytes derived from human pluripotent stem cells. *Nat Protoc.* 2014;9(6):1514–31.
- Sun J, Huang Y, Gong J, Wang J, Fan Y, Cai J, et al. Transplantation of hPSC-derived pericyte-like cells promotes functional recovery in ischemic stroke mice. *Nat Commun.* 2020;11(1):5196.

17. Faal T, Phan DTT, Davtyan H, Scarfone VM, Varady E, Blurton-Jones M, et al. Induction of mesoderm and neural crest-derived pericytes from human pluripotent stem cells to study blood-brain barrier interactions. *Stem Cell Rep.* 2019;12(3):451–60.
18. Daniszewski M, Senabouth A, Liang HH, Han X, Lidgerwood GE, Hernández D, et al. Retinal ganglion cell-specific genetic regulation in primary open-angle glaucoma. *Cell Genomics.* 2022;2(6):100142.
19. Fortune AJ, Taylor BV, Charlesworth JC, Burdon KP, Blackburn NB, Fletcher JL, et al. Generation and characterisation of four multiple sclerosis iPSC lines from a single family. *Stem Cell Res.* 2022;62:102828.
20. Mehta A, Lu P, Taylor BV, Charlesworth J, Cook AL, Burdon KP, et al. Generation of MNZTASi001-A, a human pluripotent stem cell line from a person with primary progressive multiple sclerosis. *Stem Cell Res.* 2021;57:102568.
21. King NE, Courtney JM, Brown LS, Foster CG, Cashion JM, Attrill E, et al. Pharmacological PDGFR β inhibitors imatinib and sunitinib cause human brain pericyte death in vitro. *Toxicol Appl Pharmacol.* 2022;444:116025.
22. Courtney JM, Morris GP, Cleary EM, Howells DW, Sutherland BA. An automated approach to improve the quantification of pericytes and microglia in whole mouse brain sections. *eNeuro.* 2021;8(6).
23. Neuhaus AA, Couch Y, Sutherland BA, Buchan AM. Novel method to study pericyte contractility and responses to ischaemia in vitro using electrical impedance. *J Cereb Blood Flow Metab.* 2017;37(6):2013–24.
24. Brown LS, King NE, Courtney JM, Gasperini RJ, Foa L, Howells DW, et al. Brain pericytes in culture display diverse morphological and functional phenotypes. *Cell Biol Toxicol.* 2023.
25. Hibbs E, Love S, Miners JS. Pericyte contractile responses to endothelin-1 and A β peptides: assessment by electrical impedance assay. *Front Cell Neurosci.* 2021;15.
26. Bergers G, Song S. The role of pericytes in blood-vessel formation and maintenance. *Neuro Oncol.* 2005;7(4):452–64.
27. Liu J, He L, Muhl L, Mocci G, Gustavsson S, Buyandelger B, et al. A human cell type similar to murine central nervous system perivascular fibroblasts. *Exp Cell Res.* 2021;402(2):112576.
28. Armulik A, Genové G, Betsholtz C. Pericytes: developmental, physiological, and pathological perspectives, problems, and promises. *Dev Cell.* 2011;21(2):193–215.
29. Sweeney MD, Ayyadurai S, Zlokovic BV. Pericytes of the neurovascular unit: key functions and signaling pathways. *Nat Neurosci.* 2016;19(6):771–83.
30. Canfield SG, Stebbins MJ, Faubion MG, Gastfriend BD, Palecek SP, Shusta EV. An isogenic neurovascular unit model comprised of human induced pluripotent stem cell-derived brain microvascular endothelial cells, pericytes, astrocytes, and neurons. *Fluids Barriers CNS.* 2019;16(1):25.
31. Linville RM, Sklar MB, Grifno GN, Nerenberg RF, Zhou J, Ye R, et al. Three-dimensional microenvironment regulates gene expression, function, and tight junction dynamics of iPSC-derived blood-brain barrier microvessels. *Fluids Barriers CNS.* 2022;19(1):87.
32. Mesentier-Louro LA, Suhy N, Broekaart D, Bula M, Pereira AC, Blanchard JW. Modeling the blood-brain barrier using human-induced pluripotent stem cells. *Methods Mol Biol.* 2023;2683:135–51.
33. Bosworth A, Griffin C, Chakhoyan A, Sagare AP, Nelson AR, Wang Y, et al. Molecular signature and functional properties of human pluripotent stem cell-derived brain pericytes. *bioRxiv.* 2023:2023.06.26.546577.
34. Alarcon-Martinez L, Yilmaz-Ozcan S, Yemisci M, Schallek J, Kiliç K, Can A, et al. Capillary pericytes express α -smooth muscle actin, which requires prevention of filamentous-actin depolymerization for detection. *Elife.* 2018;7.
35. Hartmann DA, Berthiaume A-A, Grant RI, Harrill SA, Koski T, Tieu T, et al. Brain capillary pericytes exert a substantial but slow influence on blood flow. *Nat Neurosci.* 2021;24(5):633–45.
36. Hill RA, Tong L, Yuan P, Murikinati S, Gupta S, Grutzendler J. Regional blood flow in the normal and ischemic brain is controlled by arteriolar smooth muscle cell contractility and not by capillary pericytes. *Neuron.* 2015;87(1):95–110.
37. Beard DJ, Brown LS, Sutherland BA. The rise of pericytes in neurovascular research. *J Cereb Blood Flow Metab.* 2020;40(12):2366–73.
38. Yamazaki T, Mukoyama YS. Tissue specific origin, development, and pathological perspectives of pericytes. *Front Cardiovasc Med.* 2018;5:78.
39. Yamazaki T, Nalbandian A, Uchida Y, Li W, Arnold TD, Kubota Y, et al. Tissue myeloid progenitors differentiate into pericytes through TGF- β signaling in developing skin vasculature. *Cell Rep.* 2017;18(12):2991–3004.
40. Edgar R, Domrachev M, Lash AE. Gene Expression Omnibus: NCB1 gene expression and hybridization array data repository. *Nucleic Acids Res.* 2002;30(1):207–10.

Publisher's Note

Springer Nature remains neutral with regard to jurisdictional claims in published maps and institutional affiliations.